

## Publication II

Petri Rönnholm, Hannu Hyypä, Petteri Pöntinen, Henrik Haggrén, and Juha Hyypä. 2003. A method for interactive orientation of digital images using backprojection of 3D data. *The Photogrammetric Journal of Finland*, volume 18, number 2, pages 58-69.

© 2003 by authors

## A METHOD FOR INTERACTIVE ORIENTATION OF DIGITAL IMAGES USING BACKPROJECTION OF 3D DATA

Petri Rönnholm<sup>1</sup>, Hannu Hyypä<sup>1</sup>, Petteri Pöntinen<sup>1</sup>,  
Henrik Haggrén<sup>1</sup> and Juha Hyypä<sup>2</sup>

<sup>1</sup>Helsinki University of Technology, Institute of Photogrammetry and Remote Sensing

<sup>2</sup>Finnish Geodetic Institute, Department of Remote Sensing and Photogrammetry

petri.ronnholm@hut.fi, hannu.hyypa@hut.fi, petteri.pontinen@hut.fi,  
henrik.haggren@hut.fi and juha.hyypa@fgi.fi

### ABSTRACT

*This paper describes a method for interactive orientation of digital images, analyses the accuracy and gives practical examples on its use. The advantages of interactive orientation are achieved if there exists random variation in the 3D data, e.g. in the laser scanning data. The human intelligence can perceive the entity and filter out possible random inaccuracies during the registration of images and reference data. The interactive orientation is also suitable for traditional orientation tasks, when accurate 3D reference data, e.g. points or lines, exists. In this paper, examples from two test sites are applied in order to demonstrate the usability and to study the accuracy of the interactive orientation method.*

### 1. INTRODUCTION

For accurate photogrammetric measurements, the transformations between camera and target coordinate systems must be known. As well, if two different kinds of data sources are used together they must be at the same coordinate system. Traditionally, photogrammetric orientation is implemented using accurate reference points or visible features and there are several robust and effective computational methods available. If the reference data does not include clear edges or corners, e.g. when working with laser scanning data, these methods are incomprehensive. In this paper the interactive orientation method was used for the registration of laser scanning data and digital images.

Laser scanning is capable to provide 3D information of the surrounding environment with accuracy almost equivalent to traditional land surveys. The main focus research areas of laser scanning include creation of 3D city models (Haala and Brenner, 1999), single-tree-based forest inventory (Hyypä and Inkinen, 1999), analysis of the factors affecting the quality of laser scanning (Ahokas et al., 2002; Schenk, 1999) and data fusion of laser scanning and digital images. The major deficiency of the laser scanning data is that it does not allow easily accurate detection of breaklines or corner points. E.g. in building extraction, laser scanning is at its best in deriving building heights, extracting planar roof faces and ridges of the roof whereas the aerial images provides nicely breaklines, and roof and house outlines.

Digital images can be used in calibration, georeferencing and quality control of the laser data, which gives a possibility to improve the geometric accuracy of the laser data. The use of digital images together with airborne laser scanning is handled mainly concerning aerial images.

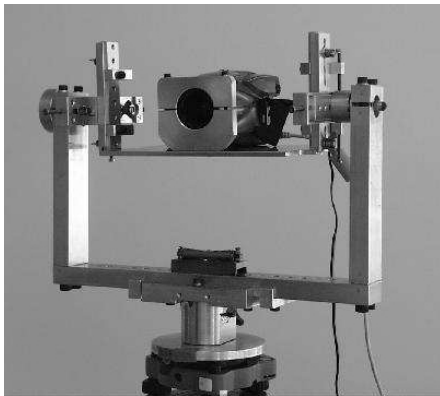
However, digital images have been used together with terrestrial laser scanning (Pfeifer and Rottensteiner, 2001) in modelling of interiors. The use of terrestrial images together with aerial laser scanner provides many new possibilities.

The aim of this paper is to present algorithms for interactive orientation between digital images and existing 3D data. The method is based on visual interpretation of the data obtained by superimposing laser scanning data on 2D images. The ability of the method is verified with real-time kinematic GPS and tacheometer observations. The paper also discusses about the potential of integrated use of airborne laser data and terrestrial digital panoramic mosaics. The interactive orientation can be done with any 3D reference data, e.g. airborne laser data, terrestrial laser data, tacheometer data, other point data and vector data.

## 2. MATERIAL

### 2.1 Panoramic Terrestrial Images

Panoramic terrestrial mosaic images were chosen because they offer wide-angle view, high resolution, and collinearity. The applied method for panoramic image creation was based on the concentric image capturing. The image capturing was carried out using a special panoramic rotation platform, in which the camera can be rotated around its projection centre (Figure 1) (Kukko, 2001; Pöntinen, 2002). The camera was calibrated in the 3D test field of the Helsinki University of Technology (HUT).



(© HUT / P. Pöntinen, A. Kukko)

Figure 1. HUT camera rotation platform enables concentric imaging.

The process of making high quality panoramic image mosaics requires derivation and elimination of lens distortions from the single images, and warping of images to a mosaic. Creation of panoramic images from concentric image sequences is presented in details e.g. in Haggrén et al. (1998) and Pöntinen (2000) and the corresponding system calibration in Hartley (1994).

Examples of the use of the depicted methods are from the test-sites in Otaniemi and Kalkkinen. The suburban test-site, university campus area Otaniemi, is located about 10 km west of Helsinki. The boreal forest test-site in Kalkkinen locates in southern Finland, 130 km north of Helsinki. The two panoramic stereo images from Kalkkinen were composed from three and two original images taken in July 1999. The dimensions of the complete images were 1539 x 3302 (Figure 5) and 1484 x 2293 pixels. Two original images were used when the panoramic image in

Otaniemi (size of (1313 x 1939)) was created in August 1999 (Figure 8). Finally, two terrestrial panoramic images, establishing a stereo pair, were created from Otaniemi in September 2002. The panoramic images, with the sizes of (9185 x 4939) (Figure 6) and (10729 x 5558) pixels, were composed from seven original images. The camera constant for all images was 1410 pixels or 9.45 mm.

## 2.2 Laser Scanning Acquisitions

The laser scanner campaigns were carried out in the Otaniemi test-site with Toposys-1 in June 2000 and with TopEye in September 2002. The test-site in Kalkkinen was measured with Toposys-1 laser scanner in June 2000. The TopoSys laser scanner is ideal for the study due to its high measurement density and steep incidence angle and the TopEye laser scanner due to the low flying height.

Toposys flights in Otaniemi were carried out with the first pulse mode from the altitude of 800 m with the average point density of 4-5 points/m<sup>2</sup>. The scan angle of the TopoSys lidar was  $\pm 7^\circ$ , wavelength was 1.54  $\mu\text{m}$  and the pulse repetition rate was 83 kHz. In Kalkkinen, the flying altitude was 400 m resulting in the average point density of 10-20 points/m<sup>2</sup>.

TopEye airborne laser scanner measures the distance between the helicopter and the terrain at a rate of 7 kHz with a wavelength of 1.064  $\mu\text{m}$ . Scan angle used was  $\pm 20^\circ$  and flying height was 200 m in Otaniemi, resulting in the average point density of 2-3 points/m<sup>2</sup>.

The accuracy of digital elevation models (DEM) in Otaniemi and the accuracy of target models in Otaniemi were studied in Hyypä and Hyypä (2003). Height errors and accuracy of laser scanning in varying terrain conditions and differences in heights were calculated. The average vertical shift between reference data and laser data was 0.08 m and the standard deviation of differences was about 0.05 m.

## 2.3 Ground Truth Data

In the Otaniemi test-site (2.5 x 3.5 km), the ground truth data was recorded during December 2000 and April 2002 in co-operation with the Finnish Geodetic Institute. Coordinates of the reference points were measured using tacheometer and Leica SR530 real-time kinematic GPS receiver. Horizontal accuracy of the RTK system was verified in Bilker and Kaartinen (2001) to be about 0.015 m and the corresponding value for vertical accuracy was 0.02 m for relatively open areas. Altogether over 1900 RTK-points were measured, 2/3 of them were ground points and 1/3 were trees, buildings, walls, lamps etc. The camera locations were also measured.

In Kalkkinen the set of signalised reference points were measured using tacheometer in September 1998 and in June 2000.

## 3. INTERACTIVE ORIENTATION METHOD

This presented interactive method for the orientation of digital images is based on backprojecting existing 3D data in the image. If the orientation of an image is incorrect, superimposed data will not fit the image. With good image resolution and clear targets, even small errors are visible. By interactively changing the exterior orientation parameters, which are camera rotations and the location of the projection centre, an operator is able to fit the superimposed 3D data and can visually verify the correctness of the orientation.

The interactive orientation requires initial values for the projection centre of the camera. An initial value for the viewing direction is also useful but not so essential, because it is easy to rotate the camera 360 degrees. The demand for the accuracy depends highly on targets – how near to the correct location we have to be before the scene is recognisable. Usually, it is enough to read approximate values from the ground map. Using initial orientation values, 3D reference data is backprojected in the image with equations we will present in the Section 3.3. The operator decides visually whether it is necessary to correct either some or every of six orientation parameters. These degrees of freedom (3+3=6) are controllable with tools, which we will introduce in the Sections 3.1 and 3.2. Typically, the main concern is to find the nearest correct camera location, because it is impossible to solve final rotations before that. After every change of orientation parameters, the reference data is superimposed again in the image. This results to iterative process where shifts, rotations and backprojections follow each other until the reference data fits the image. In the Section 3.5 we will discuss the coupling of shifts and rotations with an anchor point yielding acceleration of the method.

### 3.1 Rotating Image

The 3D-rotation matrix must be solved for image orientation. In the case of interactive orientation, it is necessary to be able to control the elements of the rotation matrix in a sensible manner. A 3D-rotation matrix  $R$  from the camera coordinate system  $x$  to the ground coordinate system  $X$  can be written

$$X = Rx = \begin{bmatrix} r_{11} & r_{12} & r_{13} \\ r_{21} & r_{22} & r_{23} \\ r_{31} & r_{32} & r_{33} \end{bmatrix} x, \quad (1a)$$

which is usually constructed with rotations around camera coordinate axes (omega ( $\omega$ ), phi ( $\varphi$ ), kappa ( $\kappa$ )) or with azimuth ( $\alpha$ ), tilt ( $\nu$ ) and swing ( $\kappa$ ) (Figure 2) when

$$\begin{array}{ll} r_{11} = \cos \varphi \cos \kappa & r_{11} = \cos \alpha \cos \kappa - \sin \alpha \cos \nu \sin \kappa \\ r_{12} = -\cos \varphi \sin \kappa & r_{12} = -\cos \alpha \sin \kappa + \cos \alpha \cos \nu \cos \kappa \\ r_{13} = \sin \varphi & r_{13} = \sin \alpha \sin \nu \\ r_{21} = \cos \omega \sin \kappa + \sin \omega \sin \varphi \cos \kappa & r_{21} = \sin \alpha \cos \kappa + \cos \alpha \cos \nu \sin \kappa \\ r_{22} = \cos \omega \cos \kappa - \sin \omega \sin \varphi \sin \kappa & r_{22} = -\sin \alpha \sin \kappa + \cos \alpha \cos \nu \cos \kappa \\ r_{23} = -\sin \omega \cos \varphi & r_{23} = -\cos \alpha \sin \nu \\ r_{31} = \sin \omega \sin \kappa - \cos \omega \sin \varphi \cos \kappa & r_{31} = \sin \nu \sin \kappa \\ r_{32} = \sin \omega \cos \kappa + \cos \omega \sin \varphi \sin \kappa & r_{32} = \sin \nu \cos \kappa \\ r_{33} = \cos \omega \cos \varphi & r_{33} = \cos \nu \end{array} \quad (1b, 1c)$$

All the rotations in equations 1b and 1c are defined to be positive to the clock-wise direction.

Being analogical to manual camera operations, “azimuth, tilt, and swing” -system tends to be easier understandable and predictable in its behaviour with terrestrial images.

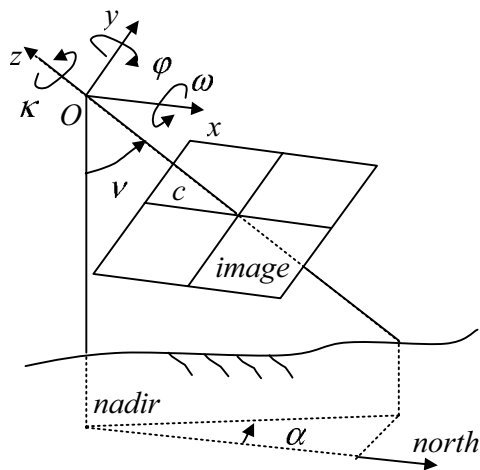


Figure 2. Typical rotations: around the axes of the camera coordinate system ( $\omega$ ,  $\phi$ ,  $\kappa$ ) or azimuth, tilt and swing ( $\alpha$ ,  $\nu$ ,  $\kappa$ ).

### 3.2 Moving Camera Location

Camera location must be found or known in order to solve the correct 3D rotations of a camera interactively. Shifts in the direction of either ground coordinate system axes or image coordinate system axes can be applied. Both methods have their own benefits. If the image plane is not parallel to either ground coordinate system axis, it might be difficult to predict how X- or Y-shifts effect to an image orientation. The Z-direction is easier to understand and to handle, however. If shifts along the camera coordinate system are used, it is easier to realize how changes effect to the view. Movements can be named: left, right, up, down, forward and backward (Figure 3). If a camera has tilt or swing, any movement affects to more than one ground coordinate direction.

The directions of camera coordinate system axes can be found directly from a 3D rotation matrix. The first column of a 3D rotation matrix (eq. 1a) is a unit vector describing the direction of x-axis of the camera coordinate system in the ground coordinate system. The second column does the same thing for y-axis and the third column for z-axis. Shifts of the projection center of the camera, or any 3D point ( $X$ ,  $Y$ ,  $Z$ ) in ground coordinates, to the direction of the x-, y- or z-axis of the camera coordinate system can be written (Gruber, 2000)

$$\begin{bmatrix} X \\ Y \\ Z \end{bmatrix}_{x\text{-shifted}} = n \begin{bmatrix} r_{11} \\ r_{21} \\ r_{31} \end{bmatrix} + \begin{bmatrix} X \\ Y \\ Z \end{bmatrix}_{\text{original}}, \quad \begin{bmatrix} X \\ Y \\ Z \end{bmatrix}_{y\text{-shifted}} = n \begin{bmatrix} r_{12} \\ r_{22} \\ r_{32} \end{bmatrix} + \begin{bmatrix} X \\ Y \\ Z \end{bmatrix}_{\text{original}}, \quad (2a, 2b, 2c)$$

$$\begin{bmatrix} X \\ Y \\ Z \end{bmatrix}_{z\text{-shifted}} = n \begin{bmatrix} r_{13} \\ r_{23} \\ r_{33} \end{bmatrix} + \begin{bmatrix} X \\ Y \\ Z \end{bmatrix}_{\text{original}}.$$

The coefficients ( $r_{11} \dots r_{33}$ ) are elements of 3D rotation matrix (eq. 1). The parameter  $n$  in equations 2a, b and c defines the amount of shift in ground coordinate system units.

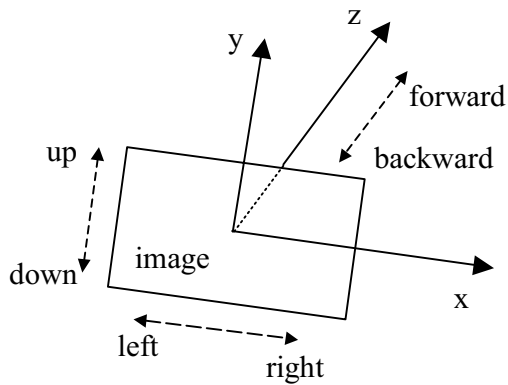


Figure 3. When shifts are made along some camera coordinate axis, movements can be called: left, right, up, down, forward, and backward.

### 3.3 Backprojection of Laser Scanning Data

When changes are applied to the rotations or to the location of the camera, the laser scanning data must again be superimposed on the image using current orientation parameters in order to see the result. The backprojection of a 3D point onto an image is calculated by the collinearity equations:

$$\begin{aligned} x &= -c \frac{r_{11}(X - X_0) + r_{21}(Y - Y_0) + r_{31}(Z - Z_0)}{r_{13}(X - X_0) + r_{23}(Y - Y_0) + r_{33}(Z - Z_0)} + x_0 \\ y &= -c \frac{r_{12}(X - X_0) + r_{22}(Y - Y_0) + r_{32}(Z - Z_0)}{r_{13}(X - X_0) + r_{23}(Y - Y_0) + r_{33}(Z - Z_0)} + y_0 \end{aligned} \quad (3)$$

where  $c$  is a camera constant, a point  $(X_0, Y_0, Z_0)$  is the projection center of a camera,  $(X, Y, Z)$  is a 3D ground point, terms  $(r_{11} \dots r_{33})$  are elements of 3D rotation matrix (see eq. 1), and  $(x_0, y_0)$  is the location of a principle point.

### 3.4 Laser Data Selection

For an interactive relative orientation, there is no need to use all available laser scanning data. Backprojecting of all the data onto an image can be quite time consuming. Using a reduced set of laser scanning data, interactive orientation becomes more practical, because the visual response of change of orientation parameters is faster. Our experience is that selection of some clearly visible features from different parts of an image is adequate.

When airborne laser scanning data is examined from a terrestrial point of view (i.e. horizontally), it might be confusing to distinguish distances from backprojected laser data, because targets close and far from the camera are mixing together. A good approach to make a side view easier to understand is to use color-coding by distance (Forsman, 2001).

### 3.5 Anchor point

Interactive orientation is a relatively slow iterative process, if both camera location and rotations are unknown, because after a shift there must be a rotation before the final result is visible. However, the use of one or several sequential anchor points can improve this method greatly. The

location of a backprojected 3D anchor point in the image plane is fixed to be at the same position despite changes in the orientation parameters (Figure 4).

An iterative method was developed to solve corrected rotations around the  $x$ - or  $y$ -axis of the camera to preserve the location of an backprojected anchor point on the image, if the projection center of the camera is moved or the image is rotated around the viewing axis. Using the omega, phi, kappa ( $\omega, \phi, \kappa$ ) -rotation system (see Figure 2) necessary corrections to omega and phi rotations can be solved, if an anchor point locates on the respective axis:

$$d\omega = \tan^{-1}\left(\frac{y_{new}}{c}\right) - \tan^{-1}\left(\frac{y_{original}}{c}\right)$$

$$d\phi = \tan^{-1}\left(\frac{x_{new}}{c}\right) - \tan^{-1}\left(\frac{x_{original}}{c}\right), \tag{4}$$

where  $c$  is a camera constant. The point  $(x_{original}, y_{original})$  is calculated using original and the point  $(x_{new}, y_{new})$  using changed orientation parameters and by applying the collinearity equations (eq. 3). These formulas are not valid, if an anchor point does not lie on the respective image axis. Fortunately, if calculation is repeated, the solution accurate enough is achieved with couple of iterations. The values of  $\omega$  and  $\phi$  are corrected on iteration rounds ( $i$ )

$$\omega_{i+1} = \omega_i \pm d\omega$$

$$\phi_{i+1} = \phi_i \pm d\phi \tag{5}$$

The signs in the equation 5 can vary depending on image attitude. The iteration can be terminated when corrections become insignificant and image coordinates of the anchor point are close enough to the original coordinates. The use of several concurrent anchor points would require extensions to presented equations.

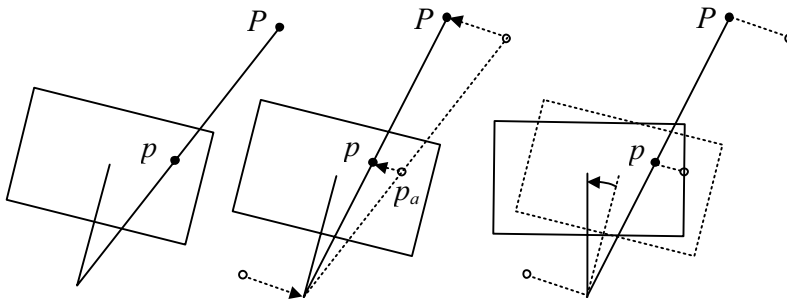


Figure 4. The location of an anchor point on the image remains because a shift of the projection centre is compensated by appropriate rotations.

#### 4. RESULTS AND DISCUSSION

In the Kalkkinen test area, there was a good possibility to test the interactive orientation method in practice, since signaled reference points measured with a tacheometer were visible from a terrestrial panoramic stereo image pair. As a reference, the exterior orientations were calculated



with traditional photogrammetric computational methods using least-squares adjustment. The left image had six and the right image five control points. No separate relative orientation was applied. The differences of the camera orientation parameters between computational and interactive methods are presented in Table 1. The results from both methods were quite alike. However, the differences in the  $X$ -direction are larger with both images. The behavior was predictable, because the images were taken mainly to this direction. The deviations of viewing directions from the  $X$ -axis were  $16^\circ$  and  $23^\circ$ . If the camera was moved forward or backward (see Figure 3), the effect on the image was much smaller compared to effects when moving left, right, up or down.

To verify both the orientations, stereo measurements were applied for common check points. The results are shown in Table 2. The main reason for a significantly worse accuracy with the first computational orientation was due to two inaccurate control points. The computational method adjusted these errors among every control point and individual residuals of observations at the image plane were not remarkable. Unfortunately, when terrestrial images were used, the effect at the ground was significant. With interactive method, it was quite easy to see that two control points did not fit with the other points and to ignore these particular points. With more correct reference points, the second computational orientation was superior, as expected, but with uncertain data the interactive method proves to be comparative, because human intelligence is able to fit the entity as a whole and to ignore unsatisfactory points. In this case, inaccurate control points could also have been identified with proper blunder detection, but with laser data, for example, these methods are not yet realistic.

Table 1. Differences of orientation parameters between computational and interactive orientation methods. The first orientation of the left image was calculated using all control points. For the second orientation inaccurate control points were removed.

	$\Delta X$	$\Delta Y$	$\Delta Z$	$\Delta\omega$ (gon)	$\Delta\phi$ (gon)	$\Delta\kappa$ (gon)
Left Image 1	-0.043 m	0.017 m	0.005 m	0.103	-0.052	0.204
Left Image 2	0.014 m	-0.017 m	-0.004 m	-0.043	0.015	-0.085
Right Image	-0.053 m	-0.012 m	0.019 m	-0.027	-0.023	0.050

Table 2. Differences between check points and stereo measurements. When terrestrial images are used, the errors of orientations cause larger errors in stereo measurements, if the point locates far from the camera.

Point	1 <sup>st</sup> computational orientation All control points			2 <sup>nd</sup> computational orientation Inaccurate control points eliminated			Interactive orientation			Point distance from 1 <sup>st</sup> camera (m)
	$\Delta X$ (m)	$\Delta Y$	$\Delta Z$	$\Delta X$	$\Delta Y$	$\Delta Z$	$\Delta X$	$\Delta Y$	$\Delta Z$	
1	0.010	0.003	-0.005	-0.007	-0.001	0.008	-0.019	-0.014	0.007	27.69
2	0.052	0.066	0.010	0.013	0.015	0.008	-0.054	-0.082	0.043	52.44
3	0.159	0.111	-0.022	-0.002	0.011	0.011	0.060	0.030	-0.019	56.26
4	0.658	0.628	-0.039	0.023	0.011	0.005	0.157	0.112	-0.038	98.77
Mean	0.220	0.202	-0.014	0.007	0.009	0.008	0.036	0.012	-0.007	
RMSE	0.340	0.321	0.023	0.014	0.011	0.008	0.089	0.071	0.030	

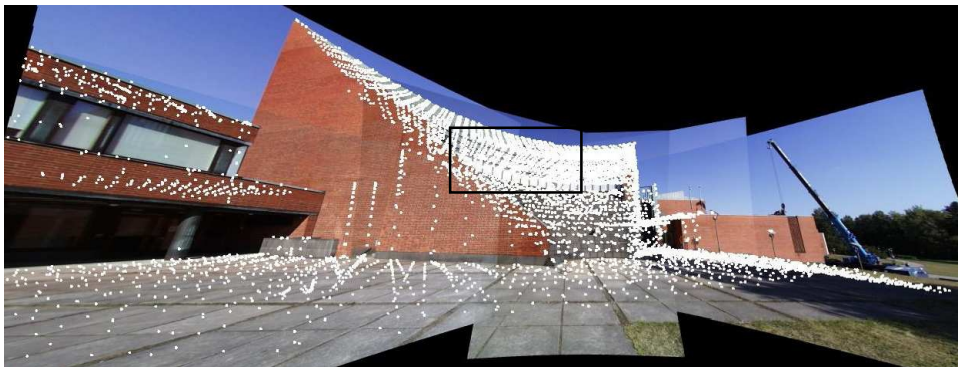
When interactive relative orientation between terrestrial images and airborne laser scanning data was examined in the Kalkkinen test-site, the relative orientation backprojected laser scanning points did fit amazingly well with the scene, although the orientation was done purely using some

tree canopies of the laser data as a reference data. In Figure 5 the laser scanning data from the year 2000 is backprojected onto the image.



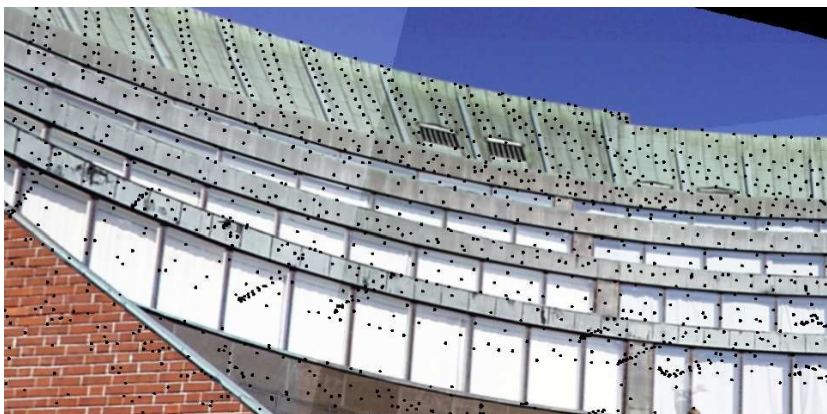
(© HUT / P. Rönnholm)

Figure 5. Laser scanning data is backprojected onto the image. The orientation was done using only tree canopies as a reference data.



(© HUT / P. Rönnholm)

Figure 6. Overview of interactively oriented terrestrial panoramic image and backprojected laser scanning data. A more detailed sub-image of the same image and laser data is presented in Figure 7.



(© HUT / P. Rönnholm)

Figure 7. Resolution of panoramic image allows detailed views. The colour of superimposed laser points has been changed from the Figure 6 to enhance the visibility.

Natural targets, such as trees and bushes, are not stable although the great redundancy of thousands of laser points increases the robustness. The quality of the interactive relative orientation method was examined in a steadier environment in Otaniemi. Two terrestrial

panoramic images were oriented interactively using a selected set of laser data. An overall image (Figure 6) depicts, how the backprojected laser scanning data complies with the image after orientation. A more detailed example from the same image and laser data is presented in Figure 7.

After the interactive orientation, the obtained camera locations were compared to the locations measured by RTK GPS (Table 3). Comparison reveals that the differences in heights between these two sources were minor. The result was as expected, since the imaging geometry is strong for this direction. Planimetric differences were slightly larger. The error was caused partly by inaccuracies with interactive orientation method, but also by some shifts between RTK-measurements and laser scanning data. It was not possible to fit the laser scanning data accurately with the images using RTK-derived camera locations.

Table 3. Comparison between RTK reference measurements and interactively oriented camera locations.

	$\Delta X_0$	$\Delta Y_0$	$\Delta Z_0$
Image 1	-0.215 m	-0.141 m	0.012 m
Image 2	-0.129 m	-0.078 m	-0.038 m



(© HUT / P. Rönnholm)

Figure 8. White spots are scanned from 800 m with the pulse repetition rate of 83 kHz (airborne TopoSys-1) and black points are scanned from 200 m at the rate of 7 kHz scanning rate (helicopter-borne TopEye).

The relative orientation of terrestrial images and laser scanning data enables new applications. One example is presented in Figure 8, where two laser scanner sets from different data sources was backprojected onto the same image. This kind of procedure gives an excellent opportunity to inspect the behavior of different laser sources. For example, the response of the lasers from a traffic sign is quite different. The differences can be due to different scanning mechanism, different flight altitude, different pulse density or any other technical parameter. It was also shown that some trees or branches have been cut between the acquisitions. Interesting subjects would also be examining laser beam reflectance from different surface materials, conforming internal quality of laser scanning data, collating different scanning strips and detecting temporal changes of the target.

The work with this interactive orientation method requires adequate tools. According to our experiences the inhibitive problem is that the final result due to shifts in the camera location is not clearly visible until the rotations are also changed. Therefore, it is more difficult to predict, how much the values should be changed at time. The use of an anchor point is a valuable tool to partially solve this problem. However, if a laser point is used as an anchor point, it is usually necessary to change it during the interactive orientation. In some cases, some pre-knowledge about the camera location or rotations is known and the interactive orientation method is fast and

easy to handle. Table 4 accumulates some typical cases with interactive orientation method and describes the level of user-friendliness. A rule of thumb with interactive orientation is that it is usually relatively fast and easy to find a coarse orientation, but the fine-tuning requires carefulness and longer time.

Table 4. Applicability of the interactive orientation method in different cases.

Properties:	Usefulness:
Shifts along ground coordinate system axes	Slow, difficult to handle
Shifts along image coordinate system axes	Faster, but still difficult to handle
Shifts along image coordinate system axes + anchor point(s)	Much faster, easier to handle
Known camera location	Fast and easy
Known camera rotations	Fast and easy

## 5. CONCLUSIONS

We have presented an interactive relative orientation method feasible for versatile applications. The method was demonstrated with panoramic terrestrial digital images, known 3D points and airborne laser scanning data. Using accurate 3D points or vector data, there are more efficient and accurate methods to solve image orientations, but interactive orientation is also feasible due to its fastness and robustness. Therefore, interactive orientation is also feasible when merging laser scanner and image data. The laser scanner data does not easily provide accurate breaklines or corner points, whereas human intelligence is able to adjust laser data quite easily with images, if the scene contains enough identifiable features.

The accuracy of the carefully performed interactive orientation is good. Only the direction of the viewing axis is less accurate due the weaker imaging geometry. The problem can be overcome by taking two images with perpendicular viewing directions. In imaging planning, it should be taken care that enough distinguishable targets are available. The panoramic images are the most suitable due to the ultra-wide angle view.

By backprojecting laser scanning data onto the oriented image, it is easier to understand the point clouds of laser scanning. In addition, relative orientation assists to verify, if there are some internal errors, discontinuities or gaps within laser data or if some changes have occurred in the target between acquisitions. Interactive relative orientation with laser scanning data works without additional control points or a digital terrain model. This is advantageous in areas, where it is difficult to make reference measurements.

This interactive orientation method is our first, straightforward and valuable step towards more sophisticated methods for relative orientation of airborne laser scanning data and terrestrial digital images. It is expected that combined use of laser scanning data and digital images will bring additional value for mapping and image interpretation.

## 6. ACKNOWLEDGEMENTS

The authors are grateful to the Academy of Finland (project numbers 76463, 201053 and 201376) and the Jenny and Antti Wihuri Foundation for financial support.

## 7. REFERENCES

- Ahokas, E., H. Hyypä, J. Hyypä, and H. Kaartinen, 2002. Analysing the effects related to the accuracy of laser scanning for digital elevation and target Models, Proceedings of Earsel, 22<sup>nd</sup> EARSeL Symposium & General Assembly, June 4 - 6, 2002, Prague, Czech Republic.
- Bilker, M. and H. Kaartinen, 2001. The Quality of Real-Time Kinematic (RTK) GPS Positioning. Reports of the Finnish Geodetic Institute 2001:1, Kirkkonummi.
- Forsman, P., 2001. Three dimensional localization and mapping of static environments by means of mobile perception. Automation technology laboratory, Helsinki University of Technology, Espoo. Series A: Research Reports No. 23. p. 145.
- Gruber, D., 2000. The Mathematics of the 3D Rotation Matrix, Presented at the Xtreme Game Developers Conference, September 30-October 1, 2000, Santa Clara, California, <http://www.makegames.com/3drotation/> (accessed 8 May 2003).
- Haala, N. and C. Brenner, 1999. Extraction of buildings and trees in urban environments, ISPRS Journal of Photogrammetry and Remote Sensing 54(2-3), 130-137.
- Haggrén, H., P. Pöntinen and J. Mononen, 1998, Cocentric image capture for photogrammetric triangulation and mapping and for panoramic visualization. IS&T/SPIE's 11th Annual Symposium on Electronic Imaging: Science and Technology, 23 to 29 January 1999, San Jose, California USA, Proc. SPIE 3641, p.17-21, 1998.
- Hartley, R., 1994. Self-Calibration from multiple views with a Rotating Camera. Lecture Notes in Computer Science, Vol. 800, Jan-Olof Eklund (Ed.), Computer Vision - ECCV '94, Springer-Verlag Berlin Heidelberg 1994.
- Hyypä J. and H. Hyypä, 2003. Laser Scanning research in Finland. Quality of laser scanning. Laserskanning och digitala bilder - idag och imorgon - mark, hus, ledningar, träd och annan vegetation i 3D. Stockholm 23.1.2003.
- Hyypä, J. and M. Inkinen, 1999. Detecting and estimating attributes for single trees using laser scanner, The Photogrammetric Journal of Finland, Vol. 16, pp. 27-42.
- Kukko, A., 2001. Digitaalikameran asemointi pallopanoraamajalustaan (Panoramic Rotation Platform for Mounting of Digital Camera, in Finnish), The Institute of Photogrammetry and Remote Sensing, Helsinki University of Technology, Espoo. 20 p.
- Pfeifer, N. and G. Rottensteiner, 2001. The Riegl laser scanner for the survey of the interiors of Schönbrunn palace. Fifth Conference on Optical 3-D Measurement Techniques. Vienna. 4.-6.10.2001.
- Pöntinen, P., 2000. On the creation of panoramic images from image sequences. XIXth Congress of the International Society of Photogrammetry and Remote Sensing, Amsterdam, 17.-23.7.2000. Amsterdam 2000, ISPRS, pp. 635-641.
- Pöntinen, P., 2002. Camera Calibration By Rotation. International Society for Photogrammetry and Remote Sensing - ISPRS Commission V, September 3-7.2002, Corfu, Greece. Pp. 585-589.
- Schenk, T., B. M. Csatho and D-C. Lee, 1999. Quality control issues of airborne laser ranging data and accuracy study in an urban area. International Archives of Photogrammetry and Remote Sensing ,32(3 W14), 101-108.